Supporting information for

Layer-by-Layer Assembly of a Metallomesogen by Dip-Pen Nanolithography

By *Boya Radha*, *Guoliang Liu*, *Daniel J. Eichelsdoerfer*, *Giridhar U. Kulkarni*, and *Chad A. Mirkin**

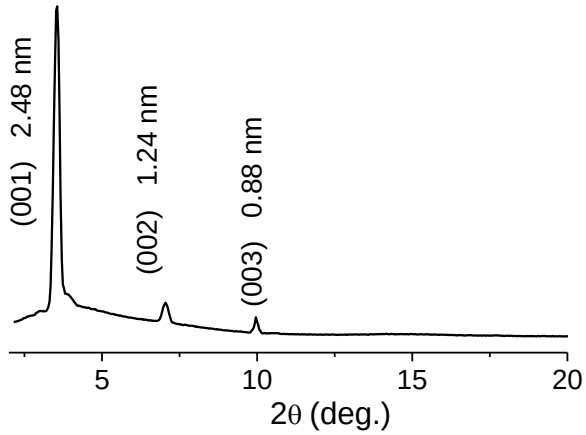

Figure S1. XRD pattern of a drop-cast Pd octylthiolate film on a glass slide.

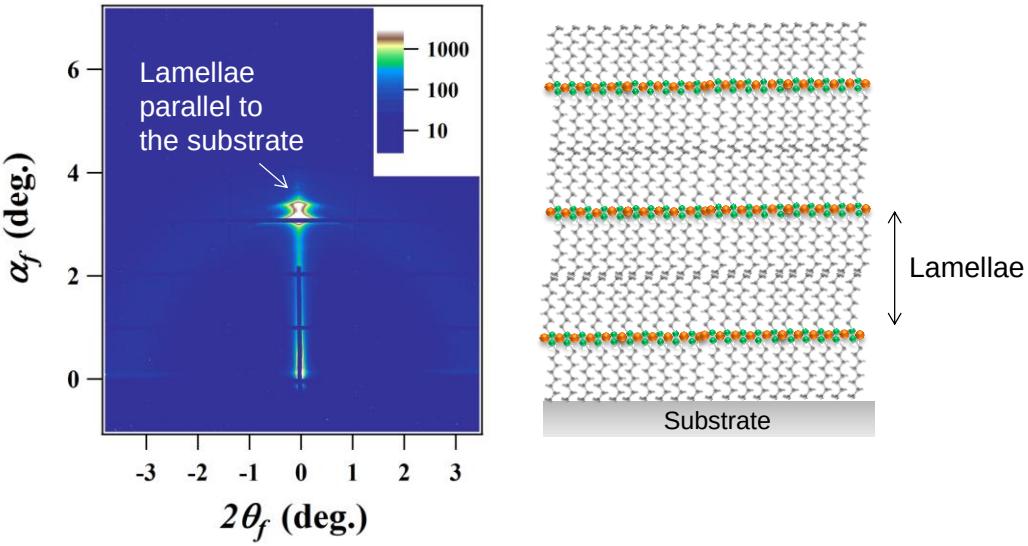

Figure S2. 2D GISAXS data from a spin-coated film of Pd octylthiolate. Strong scattering intensity in the vertical direction indicates the stacking of the lamellae parallel to the surface as

shown in the schematic. The film was prepared by spin-coating a 50 mM solution of Pd octylthiolate in toluene on a Si substrate at 2000 rpm for 60 s.

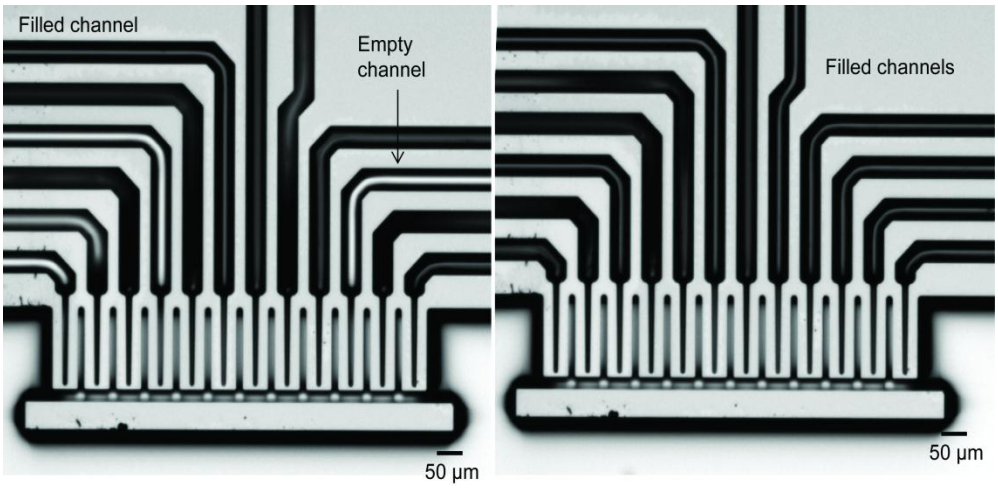

Figure S3. Optical images of the inkwell arrays with Pd octylthiolate ink in the microchannels. After all the channels are filled with ink, AFM tip arrays are brought in contact with the microchannels for inking.

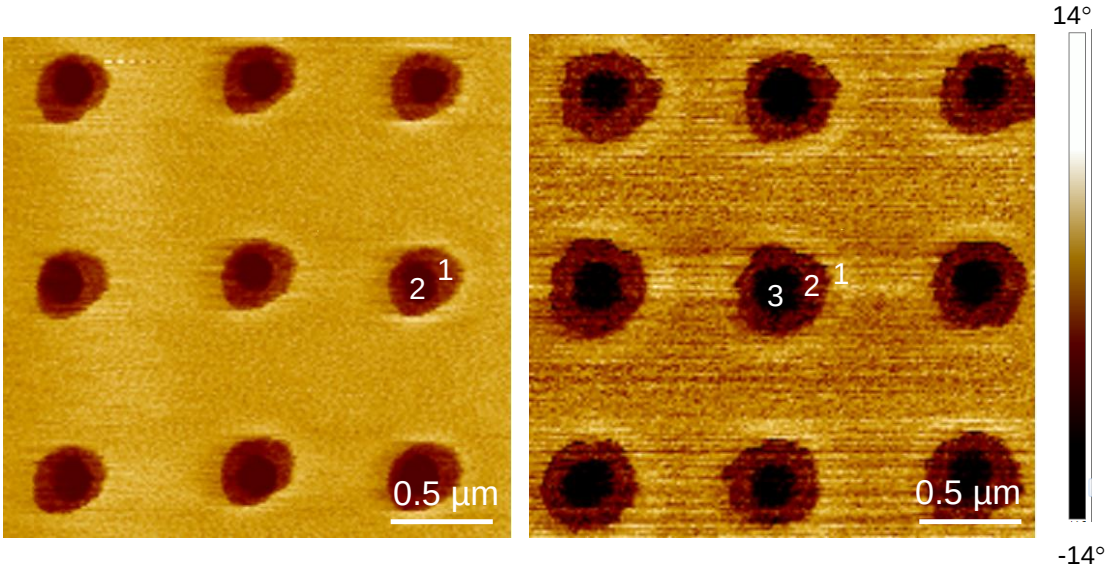

Figure S4. Phase contrast images of patterned arrays of two layers (left) and three layers (right) of Pd octylthiolate. The numbers indicating molecular layers are provided on the figure.

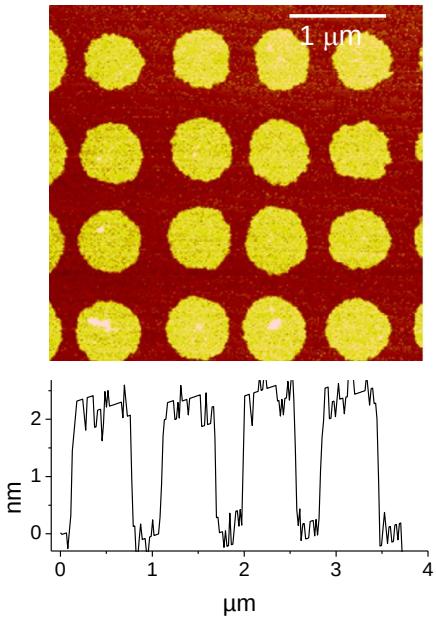

Figure S5. AFM image of the patterned Pd thiolate monolayers formed by DPN of Pd octylthiolate (10 mM ink concentration). Lower image shows a height profile of the patterned features.

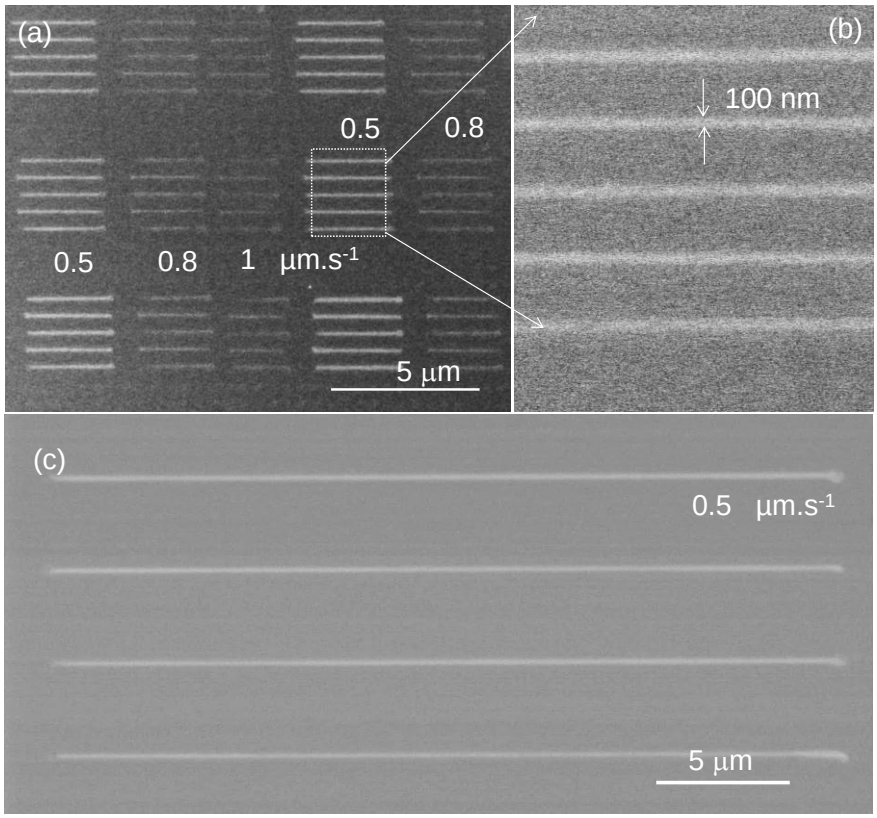

Figure S6. (a,b) SEM images of typical lines written at varying speeds (100 mM ink concentration). (c) Long contiguous lines written using the same recipe.

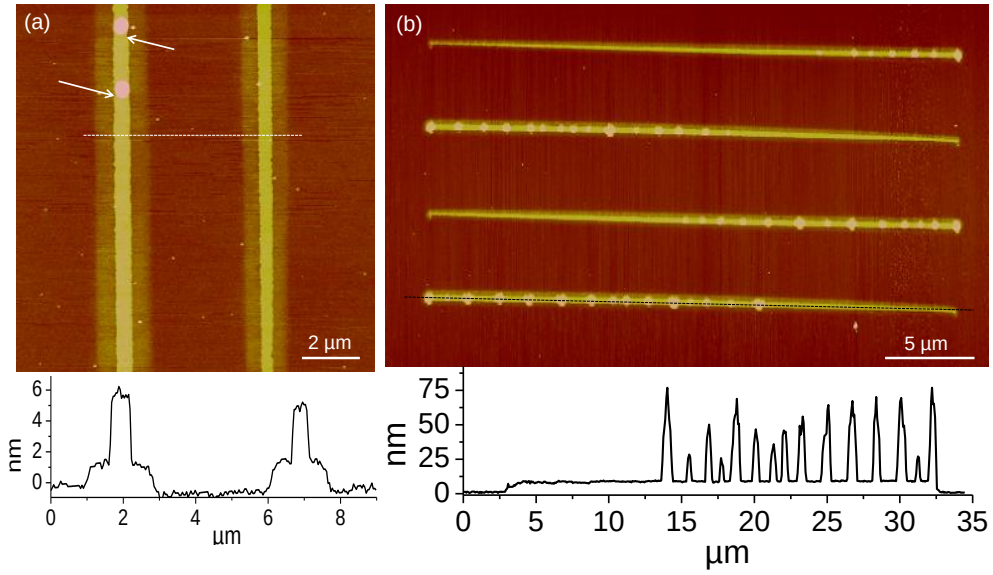

Figure S7. AFM image of Pd octylthiolate lines of (a) three-layers and (b) multi-layers, with corresponding height profiles taken along the white lines in each image. As evident in the AFM height profiles, tri-layers are difficult to obtain in a stacked manner. Note that tri-layer and multi-layer structures have non-uniform distribution of Pd octylthiolate along the length of the line, as shown by the spots of piled-up ink (arrows in (a)) along the length of the line. The ink concentration was 50 mM and write speeds were 0.3 and 0.8 µm.s^{-1} for (a) and (b), respectively.

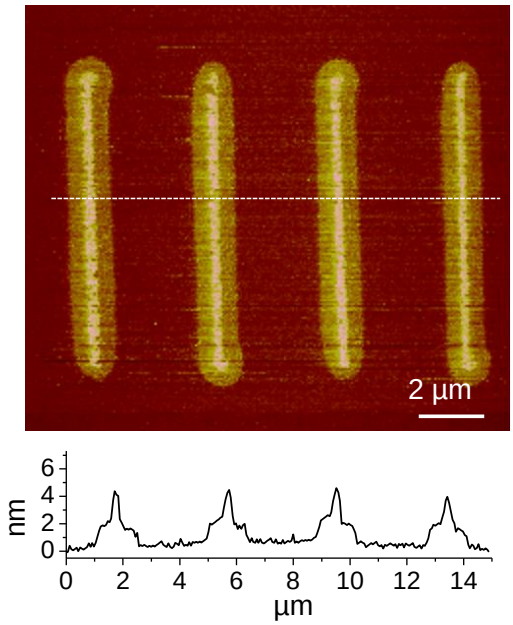

Figure S8. AFM image of the Pd octylthiolate bi-layer lines. The ink concentration was 50 mM and writing speed was 0.5 µm.s^{-1}.

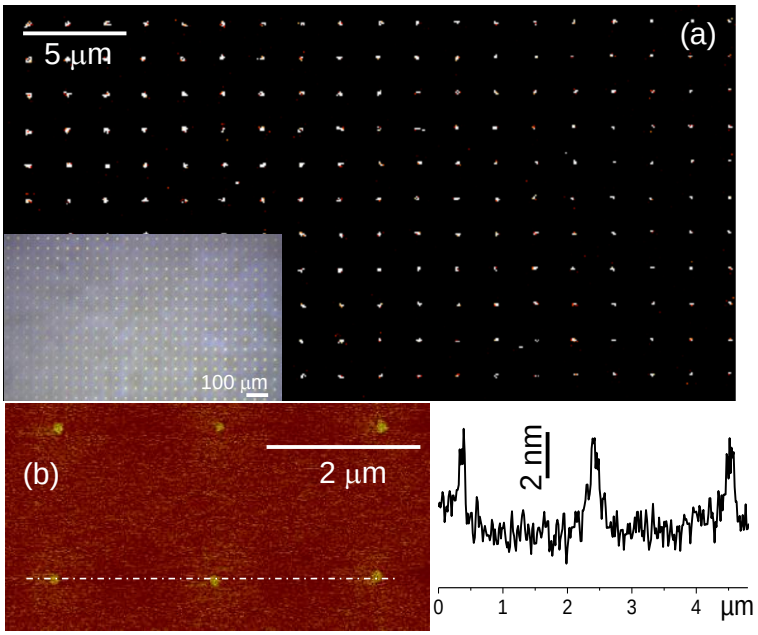

Figure S9. (a) AFM image of the patterned Pd octylthiolate dots by PPL with decreasing force from left to right. Inset shows an optical micrograph of patterns over a large area. (b) AFM of smaller features (on right-hand side in (a)) with height profile. The *z*-piezo extension was varied from -2 to -12 µm (with initial contact at $z = 0$ µm) with decreasing steps of 0.5 µm from right to left. The ink concentration employed was 100 mM and the dwell time was 100 ms.

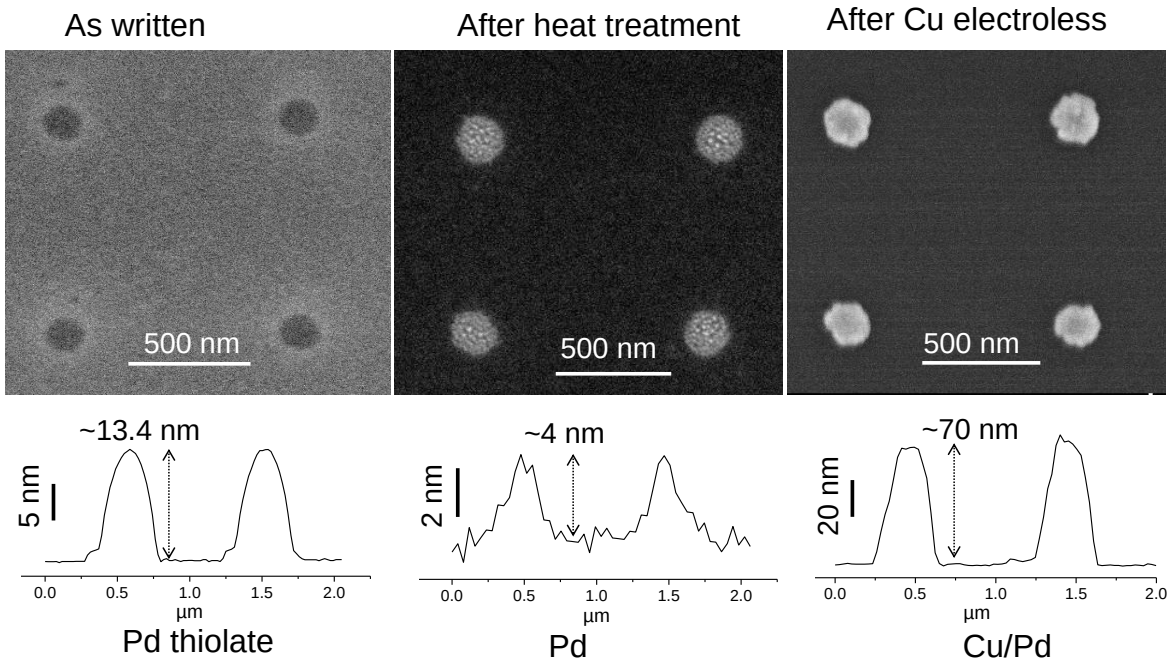

Figure S10. SEM images (upper row) and AFM height profiles (lower row) of the as-patterned Pd octylthiolate, the patterns after thermolysis and after electroless Cu deposition. The ink concentration was 100 mM and the dwell time was 0.01 s.

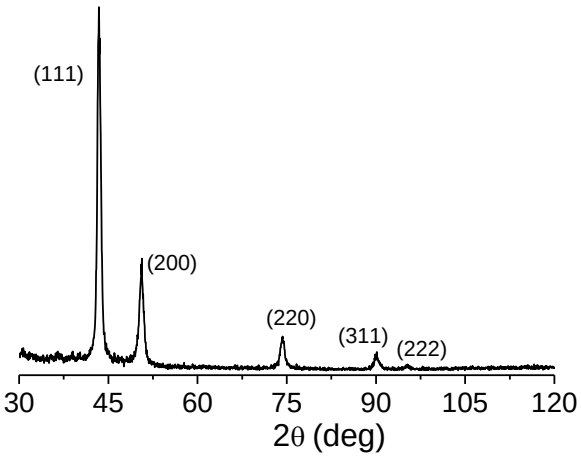

Figure S11. XRD pattern of Cu film deposited by electroless deposition on Pd. The Pd octylthiolate film was drop-cast onto a glass slide and thermolyzed at 250 °C for 1 hr, leading to a Pd film. Following this, electroless deposition of Cu (*vide supra*) was performed for ~30 s. The film appeared copper red in color.

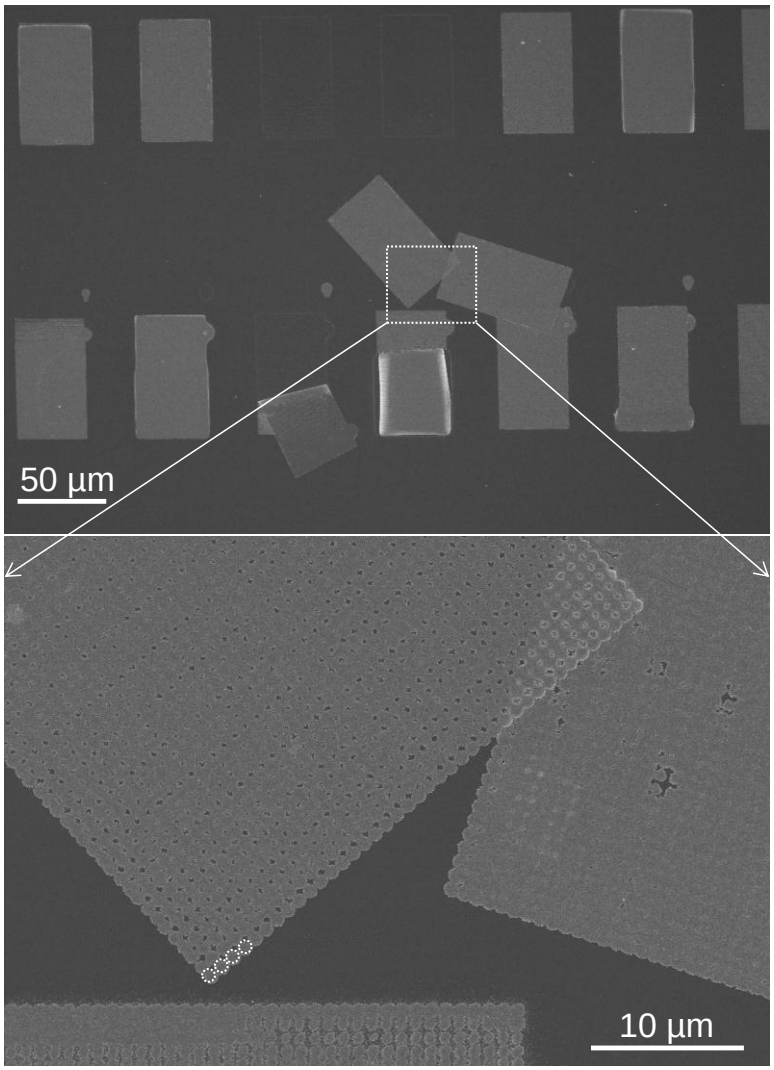

Figure S12. SEM images of Pd patterns with electrolessly deposited Cu. Prolonged electroless deposition time (> 2 min) merged the adjacent Pd seeds and the sheets delaminated from the surface (upper image). As shown in the lower image, each rectangular feature is composed of a square array of dots, which became connected due to excess Cu deposition. A few dots are circled for clarity.

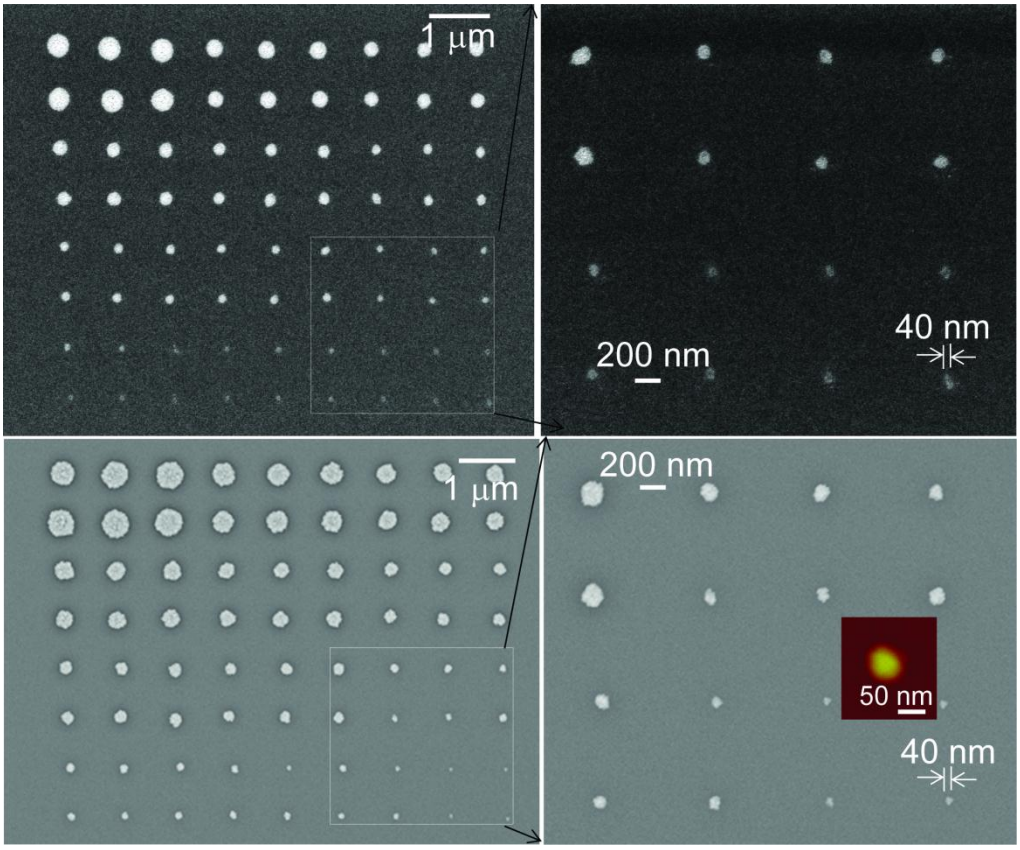

Figure S13. SEM images of the patterned Pd octylthiolate dots with varying feature size (top row), and images of the dots after electroless Cu deposition (bottom row). The inset shows an AFM image of a single Cu dot with a diameter of ~40 nm. The dwell time was varied from 1 s to 0.002 s, and the ink concentration was 100 mM. Electroless deposition of Cu was done for ~30 s.

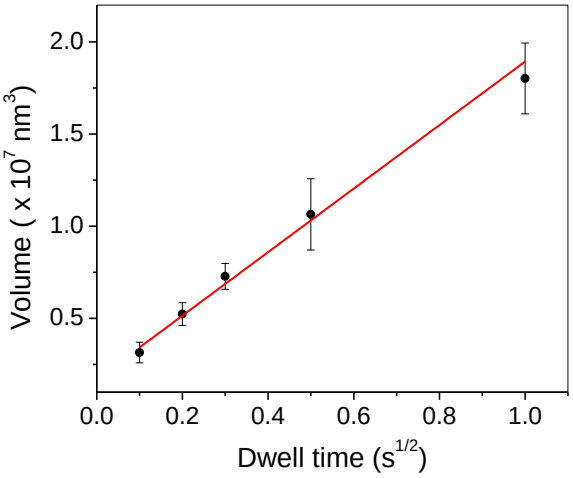

Figure S14. Square root of dwell time employed for Pd octylthiolate patterning versus volume of the resulting Cu features obtained after thermolysis and subsequent electroless Cu deposition. Pd octylthiolate concentration for this experiment was 100 mM.

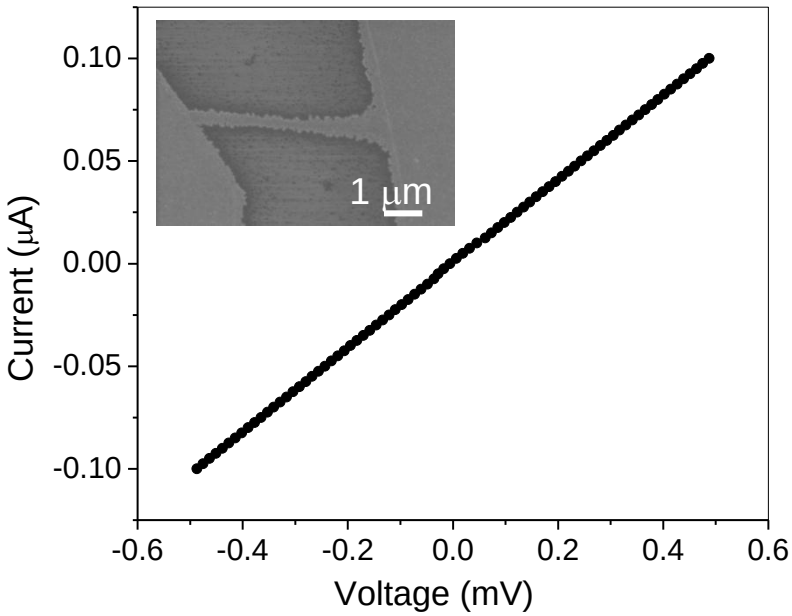

Figure S15. I-V response from Cu/Pd line with inset showing SEM image.

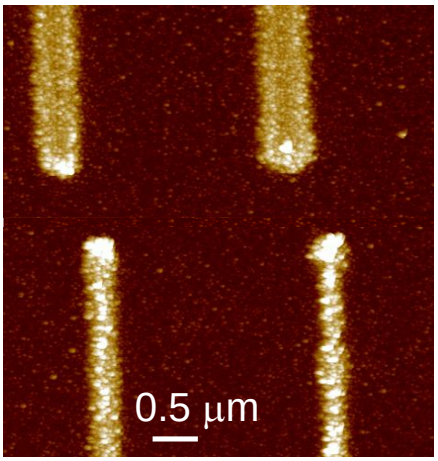

Figure S16. AFM image of Cu lines with a gap of less than 1 μm. The concentration of Pd octylthiolate ink was 100 mM. The write speed of the top and bottom lines was 0.5 and 1 μm/s respectively. After themolysis, electroless Cu deposition was done for ~30 s.

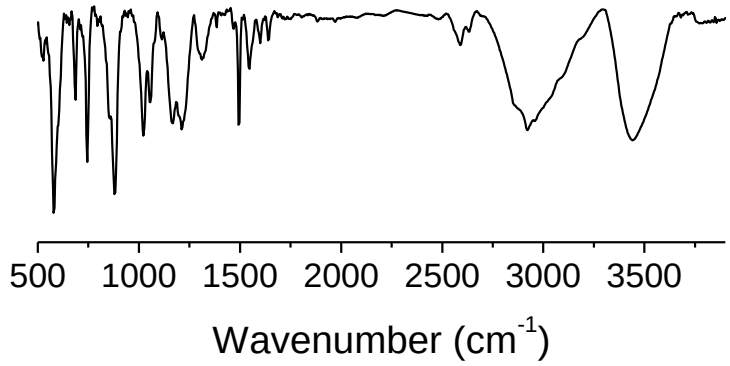

Figure S17. FTIR spectrum from electrolessly deposited PANI. The peak assignments are shown below.[1]

Wave number(cm^{-1})	Type of stretching
3444	ν(N–H) (primary amino group)
2923	Aromatic ν(C–H)
2588	CO_2
1639	N–H scissoring of primary aromatic amine
1542	Aromatic ring-stretching in substituted Phz unit
1492	Benzenoid (B) ring stretching
1465	C=C stretching of aromatic ring; N=N stretching
1384	C–N stretching in QBQ units
1311	ν(C–N) of secondary aromatic amine
1211	ν(C–N) in BBB unit; Phz-type ring
1164	N=Q=N/δ(C–H)
1056	δ(C–H) (monosubstituted ring)
1022	HSO_4^-/SO_3^- group on sulfonated aromatic ring
879	γ(C–H) (1,2,4-trisubstituted ring) (2H)/B ring deformation
744	γ (C–H) (monosubstituted or 1,2-disubstituted ring)
686	Out-of-plane ring bending (monosubstituted ring)
578	HSO_4^-

B: benzenoid ring; Q: quinonoid ring; Phz: phenazine; ν: stretching; γ: out-of-plane deformation; δ: in-plane deformation

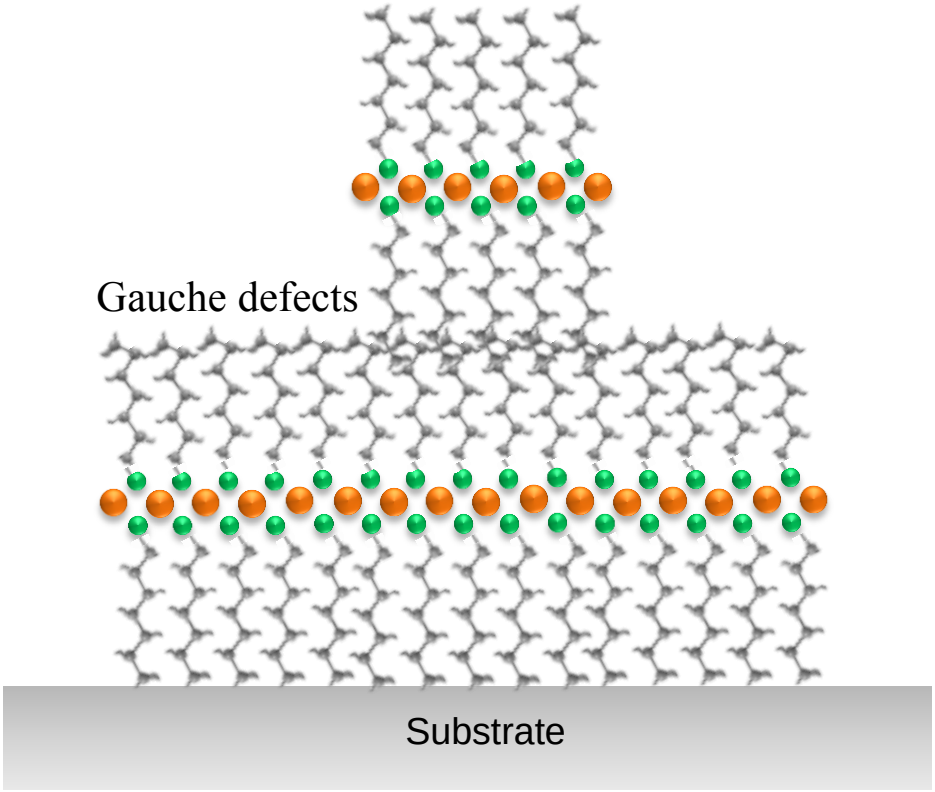

Scheme S1. Double layer Pd octylthiolate showing possible defects on the first molecular layer and interdigitation of the alkyl chains from the top and bottom layers.

1. M. Trchova, J. Stejskal, *Pure Appl. Chem.* **2011**, *83*, 1803-1817.